Electronic Supplementary Information

Silicon nitride nanopore created by dielectric breakdown with a divalent cation: deceleration of translocation speed and identification of single nucleotides

Yusuke Goto*, Kazuma Matsui, Itaru Yanagi and Ken-ichi Takeda

Center for Technology Innovation - Healthcare, Research & Development Group, Hitachi Ltd., 1-280 Higashi-Koigakubo, Kokubunji, Tokyo 185-8601, Japan

The supplementary information includes the following:

SI-1. Device structure for silicon nitride nanopore fabrication

A substrate with a silicon nitride (SiN) membrane designed for nanopore fabrication via controlled dielectric breakdown (CBD) is illustrated in Figure S1. A 100-nm-thick Si_3N_4 layer, a 150-nm-thick poly-Si layer and a 5-nm-thick Si_3N_4 layer were deposited on a Si substrate. A 500 x 500 nm^2 square hole was fabricated by dry etching, and the poly-Si layer was partially eliminated by KOH etching. The detailed procedure was described in a previous report.[1]

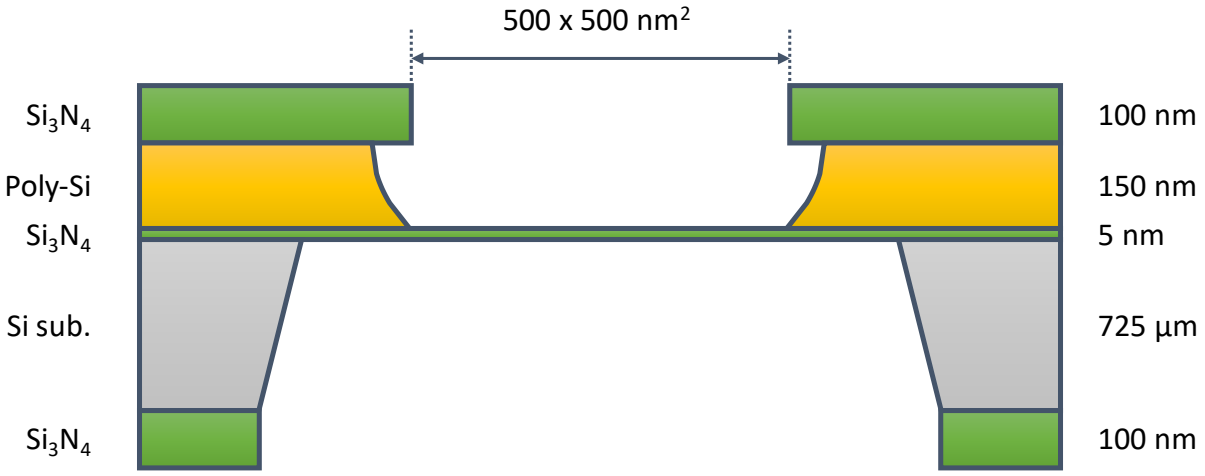

Figure S1. Schematic diagram of a substrate with a 5-nm-thick SiN membrane for nanopore fabrication via controlled dielectric breakdown.

SI-2. DNA translocation across a $CaCl_2$-CBD nanopore in $CaCl_2$ solution

We evaluated poly(dA)$_{60}$ translocation across a SiN nanopore created by CBD with 1 M $CaCl_2$ aqueous solution buffered with 10 mM Tris-HCl in the same $CaCl_2$ solution. Figure S2a and b show a typical current trace for poly(dA)$_{60}$ translocation through the nanopore and a log-scale histogram for dwell time. The most frequent dwell time was 5.1 ms (84 μs/base), which is approximately 80 times slower than the reported value (1 μs/base) for a conventional nanopore.[2–4]

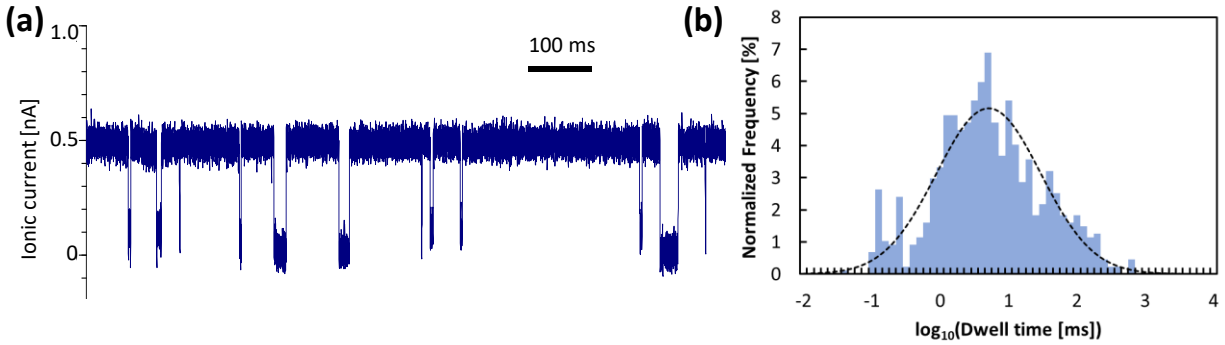

Figure S2. (a) Typical current trace for poly(dA)$_{60}$ translocation across a SiN nanopore with a diameter of 1.0 nm in 1 M $CaCl_2$ solution buffered with 10 mM Tris-HCl (pH 7.5) at 0.1 V. The nanopore was fabricated by CBD with the same 1 M $CaCl_2$/10 mM Tris-HCl buffer (pH 7.5). The data were measured at room temperature and low-pass filtered at 5 kHz. (b) The log-scaled normalized histogram of dwell time for ssDNA translocation (N=1031).

SI-3. Characteristics of a nanopore created by CBD with a divalent cation

Figure S3a shows a typical current trace of a SiN nanopore fabricated by CBD with a 1 M aqueous solution of $CaCl_2$ as a divalent cation buffered with 10 mM Tris-HCl. The stable current and linear I-V characteristics can be obtained after the exchange of the solution with 4 M CsCl/10 mM Tris-HCl aqueous solution.

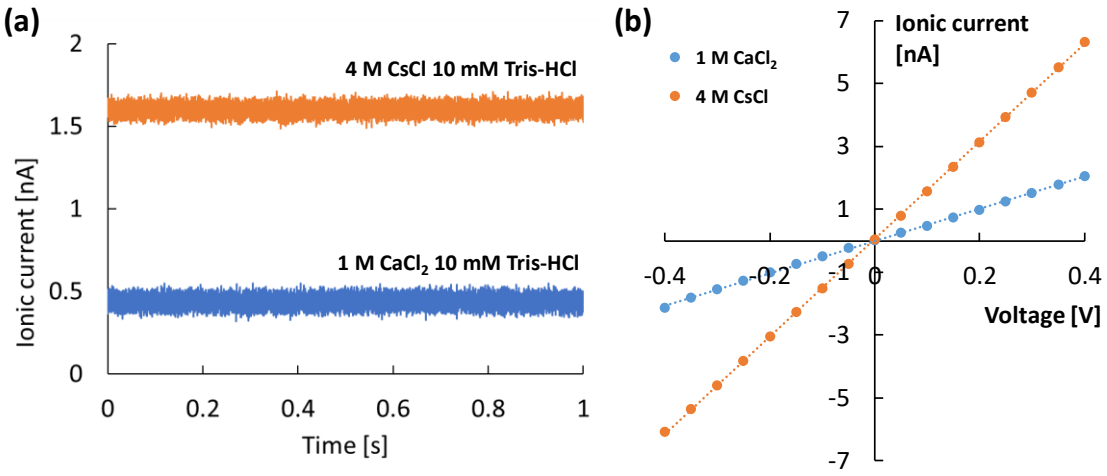

Figure S3. (a) Typical current trace of a $CaCl_2$-CBD nanopore at an applied voltage of 0.1 V under 1 M $CaCl_2$ solution buffered with 10 mM Tris-HCl at pH 7.5 (blue) or 4 M CsCl solution buffered with 10 mM Tris-HCl at pH 7.5 (orange). (b) I-V characteristics of the nanopore in 1 M $CaCl_2$ solution buffered with 10 mM Tris-HCl at pH 7.5 (blue) or 4 M CsCl solution buffered with 10 mM Tris-HCl at pH 7.5 (orange).

SI-4. Slowing effect on other sequences of ssDNA

We investigated the slowing effect of the $CaCl_2$-CBD nanopore on DNA translocation for other sequences of single-stranded DNA (ssDNA) using poly$(dA)_{60}$ and poly$((dG)_1(dA)_1(dC)_1(dT)_1)_{11}$. Figure S4 presents the normalized log-scaled histogram of dwell time for ssDNAs. These histograms are similarly well fitted by log-normal distributions with peaks at 6.0 ms (poly$(dA)_{60}$) and 6.1 ms (poly$((dG)_1(dA)_1(dC)_1(dT)_1)_{11}$). These dwell times correspond to translocation speeds of 100 μs/base (poly$(dA)_{60}$) and 140 μs/base (poly$((dG)_1(dA)_1(dC)_1(dT)_1)_{11}$). The obtained speeds are almost the same as in the case of 82-nt ssDNA described in the main text. The results indicate that the slowing effect of the $CaCl_2$-CBD nanopore effectively decreases the translocation speed of DNAs with various sequences to 100 μs/base.

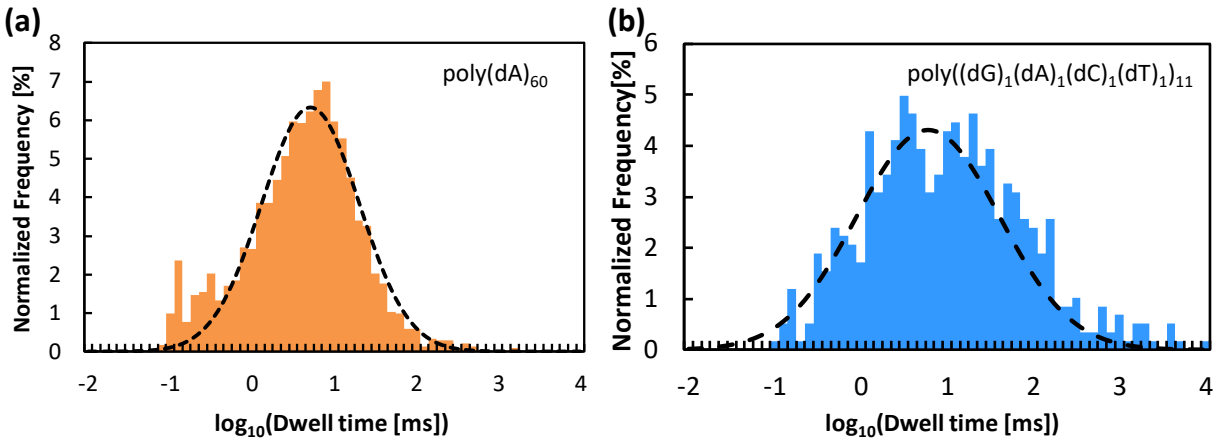

Figure S4. The log-scaled histograms of dwell time for ssDNAs with other sequences: (a) poly$(dA)_{60}$ (N=2331) and (b) poly$((dG)_1(dA)_1(dC)_1(dT)_1)_{11}$ (N=1107), using nanopores fabricated in 1 M $CaCl_2$ solution buffered with 10 mM Tris-HCl (pH 7.5) at room temperature. All data were measured at an applied voltage of 0.1 V in 4 M CsCl solution buffered with 10 mM Tris-HCl (pH 7.5).

SI-5. Effect of electrolyte concentration at DNA measurement

The electrolyte concentration at DNA measurement affects the DNA translocation speed across a $CaCl_2$-CBD nanopore. Figure S5 shows log-scaled histograms of dwell time for poly$(dA)_{60}$ in 1 M CsCl solution buffered with 10 mM Tris-HCl or 4 M CsCl solution buffered with 10 mM Tris-HCl. The most frequent dwell times are 2.1 ms (1 M CsCl) and 6.0 ms (4 M CsCl). Therefore, a 4-fold increase in the electrolyte concentration resulted in an approximately 3-fold deceleration of DNA speed. This feature is consistent with the previously reported result.[5] The use of a measurement solution with a high concentration enables not only deceleration of the DNA speed but also an increase in conductivity (1 M CsCl: 10.8 S/m, 4 M CsCl: 38.0 S/m) with an approximate 4-fold signal-to-noise ratio. Thereafter, a solution with a high concentration is preferred for DNA measurement using the $CaCl_2$-CBD nanopore. For the Debye length, we used a 1.0-nm-diameter nanopore in our experiments to investigate the slowing effect. This ultrasmall nanopore size is almost the same as the Debye length in our experiments (1 nm at 1 M CsCl solution and 0.5 nm at 4 M CsCl solution). Therefore, we considered that DNA could interact sufficiently with the adsorbed ions at the nanopore even under shorter Debye length conditions of 4 M CsCl solution.

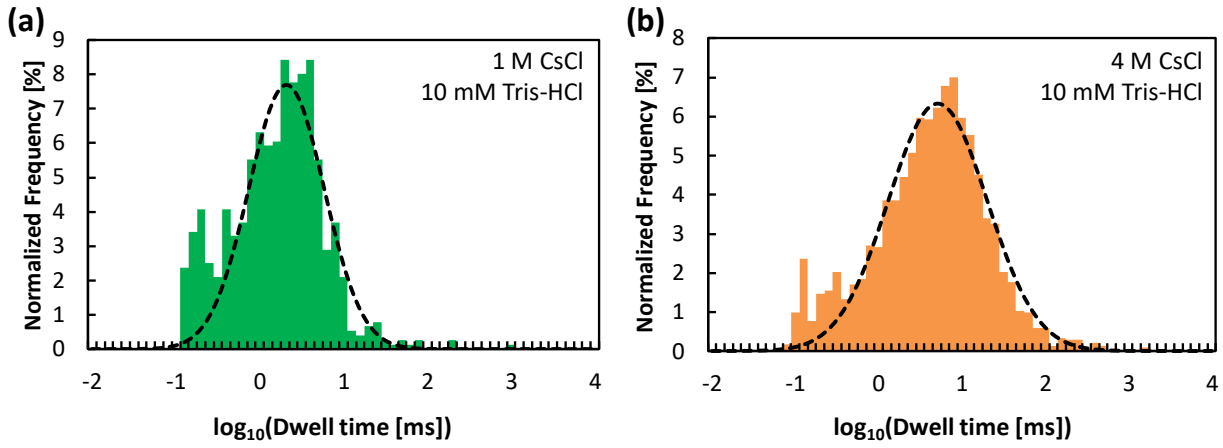

Figure S5. The log-scaled histograms of dwell time for poly(dA)$_{60}$ translocation using a different nanopore fabricated in 1 M $CaCl_2$ solution buffered with 10 mM Tris-HCl (pH 7.5) at room temperature. All data were measured at an applied voltage of 0.1 V in (a) 1 M CsCl solution buffered with 10 mM Tris-HCl buffer at pH 7.5 (N=1010) or (b) 4 M CsCl solution buffered with 10 mM Tris-HCl buffer at pH 7.5 (N=2331).

SI-6. Temperature dependence of dwell time for other DNA translocations

We evaluated the temperature dependence of dwell time for other ssDNAs (poly(dA)$_{60}$) using a $CaCl_2$-CBD nanopore. It was observed that the dwell time similarly depends on temperature. The most frequent peaks were 6.0 ms (0.1 ms/base) at 25 ^{o}C, 63 ms (1.1 ms/base) at 4 ^{o}C, 250 ms (4.2 ms/base) at -8 ^{o}C and 710 ms (12 ms/base) at -16 ^{o}C. Figure S6 shows an Arrhenius plot for poly(dA)$_{60}$ translocation. These data were also well fitted (R^2 = 0.99) by the Arrhenius law. We obtained an enthalpic barrier of 30 k_BT, which is the same order of magnitude as that for the ssDNA described in the main text.

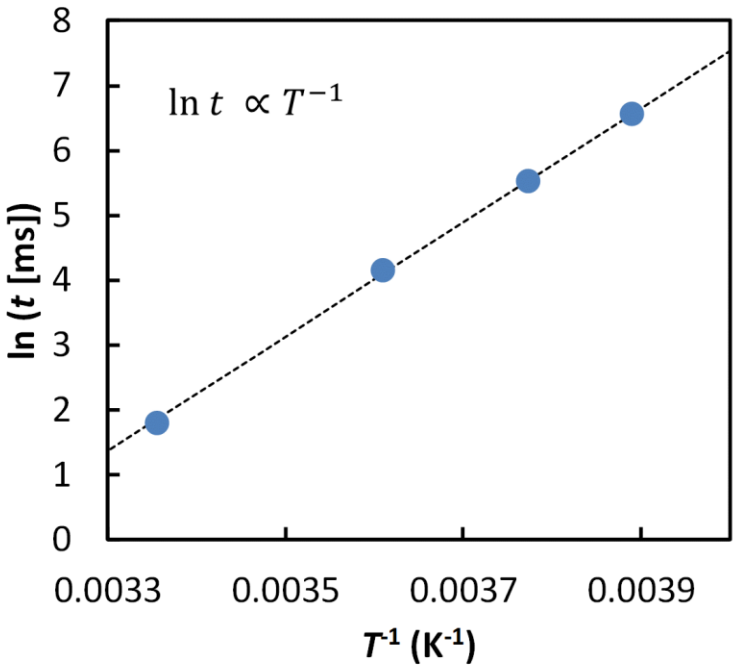

Figure S6. The Arrhenius plot for poly(dA)$_{60}$ translocation across a $CaCl_2$-CBD nanopore at an applied voltage of 0.1 V. All data were measured at various temperatures in 4 M CsCl solution buffered with 10 mM Tris-HCl at pH 7.5.

SI-7. Dependence of the slowing effect on nanopore diameter

We found an obvious dependence of the slowing effect on the diameter of nanopores. Figure S7 shows the scatter plot for poly(dA)$_{60}$ translocation time versus diameter of nanopores fabricated by CBD in 1 M $CaCl_2$ solution buffered with 10 mM Tris-HCl, 1 M CsCl solution buffered with 10 mM Tris-HCl, or 1 M HCl solution. There was a dramatic delaying effect with a boundary of 1.2 nm. DNA translocation was decelerated and tended to be almost constant when using a nanopore with a diameter smaller than 1.2 nm. However, the slowing effect could not be observed when using a nanopore with a diameter larger than 1.3 nm, even when a nanopore was created by CBD with $CaCl_2$. This transition point indicated that the minimum diameter at which ssDNA can sufficiently interact with the Ca^{2+}-adsorbed layer on the nanopore sidewall is 1.2 nm. This value matches the molecular diameter of ssDNA calculated from crystal analysis.[6] Therefore, a strong interaction between DNA and the sidewall of the nanopore begins to appear when the diameter of a nanopore is smaller than that of ssDNA. On the other hand, the DNA translocation time using a CsCl-CBD nanopore or a HCl-CBD nanopore was still short even when the diameter of the nanopore was smaller than 1.2 nm. This difference is additional evidence for the slowing effect of a $CaCl_2$-CBD nanopore.

We also evaluated the temperature dependence of poly(dA)$_{60}$ translocation time using $CaCl_2$-CBD nanopores with diameters of 1.0 nm or 1.6 nm. Figure S8 shows Arrhenius plots for both nanopores. We observed a clear temperature dependence of the DNA translocation time for the 1.0-nm diameter nanopore, while only a slight temperature dependence of the DNA translocation time was observed for the 1.6-nm diameter nanopore. The results also support that the origin of the slowing effect is the interaction between DNA and the divalent cations on the sidewall of the nanopore.

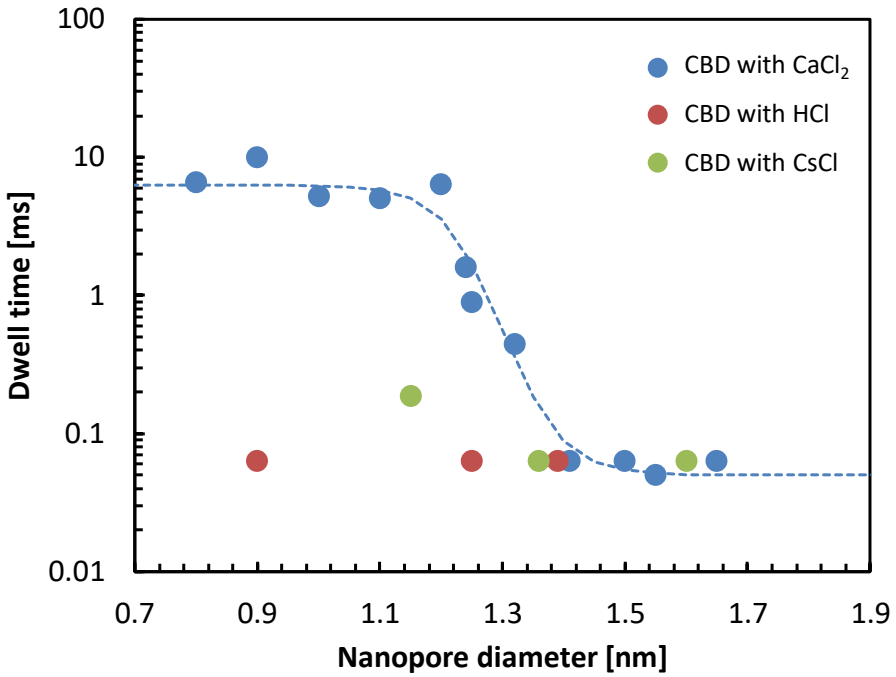

Figure S7. The scatter plot of nanopore diameter versus dwell time of ssDNA translocation across a nanopore fabricated with 1 M $CaCl_2$ solution buffered with 10 mM Tris-HCl at pH 7.5 (blue), 1 M CsCl solution buffered with 10 mM Tris-HCl at pH 7.5 (green) and 1 M HCl solution (red). All data were measured at an applied voltage of 0.1 V in 4 M CsCl solution buffered with 10 mM Tris-HCl at pH 7.5 (at room temperature). The dashed line is the fitted curve of a sigmoid function.

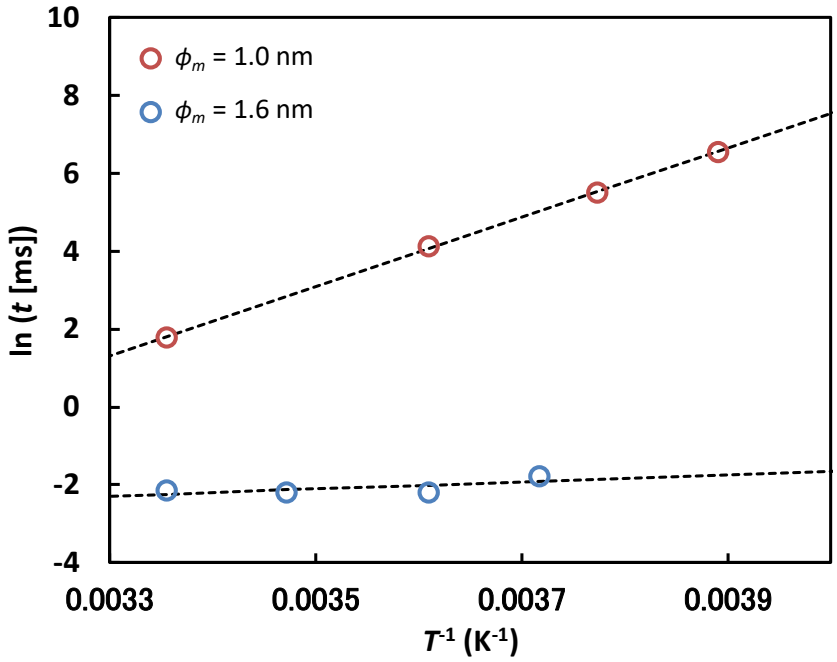

Figure S8. The Arrhenius plot for the poly(dA)$_{60}$ translocation experiment using (a) a 1.0-nm-diameter nanopore and (b) a 1.6-nm-diameter nanopore fabricated in 1 M $CaCl_2$ solution buffered with 10 mM Tris-HCl at pH 7.5. All data were measured at an applied voltage of 0.1 V in 4 M CsCl solution buffered with 10 mM Tris-HCl at pH 7.5.

SI-8. Voltage dependence of dwell time and translocation frequency

Figure S9 presents the voltage dependence of the DNA duration time, *t*, and DNA translocation frequency, *f*, for poly(dA)$_{60}$ translocation using a $CaCl_2$-CBD nanopore. Previous works have reported that the voltage dependence of ssDNA translocation time decreases exponentially[7] and that the voltage dependence of ssDNA translocation frequency increases linearly.[8] We confirmed that our $CaCl_2$-CBD nanopore behaves similarly to a conventional SiN nanopore.

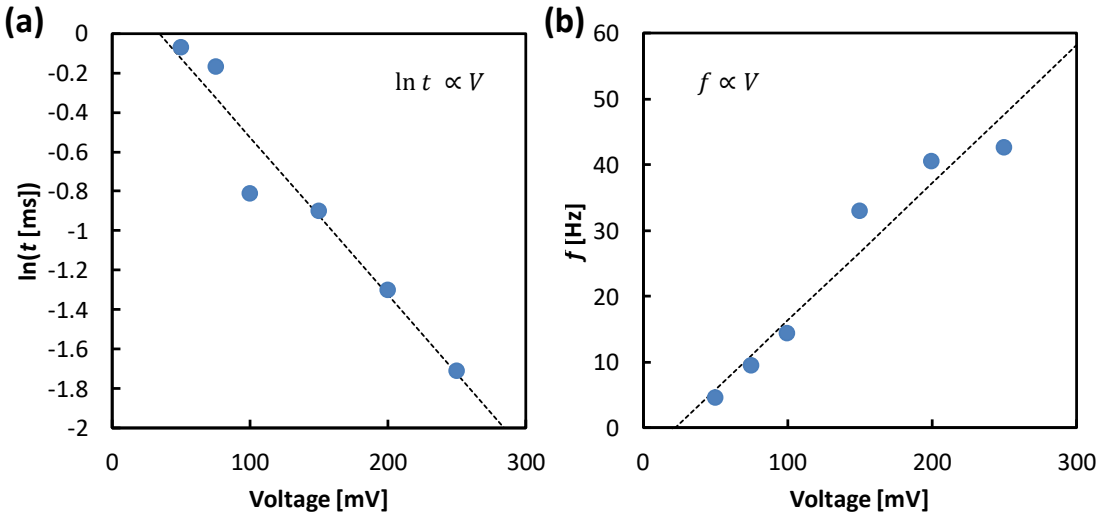

Figure S9. The voltage dependence of the dwell time and frequency of ssDNA translocation. dA$_{60}$ translocation was measured using a 1.3-nm-diameter nanopore fabricated with 1 M $CaCl_2$ solution buffered with 10 mM Tris-HCl at pH 7.5. All data were measured at room temperature in 4 M CsCl solution buffered with 10 mM at pH 7.5.

SI-9. Typical current trace for dNMP measurement

Figure S10 shows typical current traces for dNMP translocation across $CaCl_2$-CBD nanopores. Stable measurement of dNMP translocation can be performed.

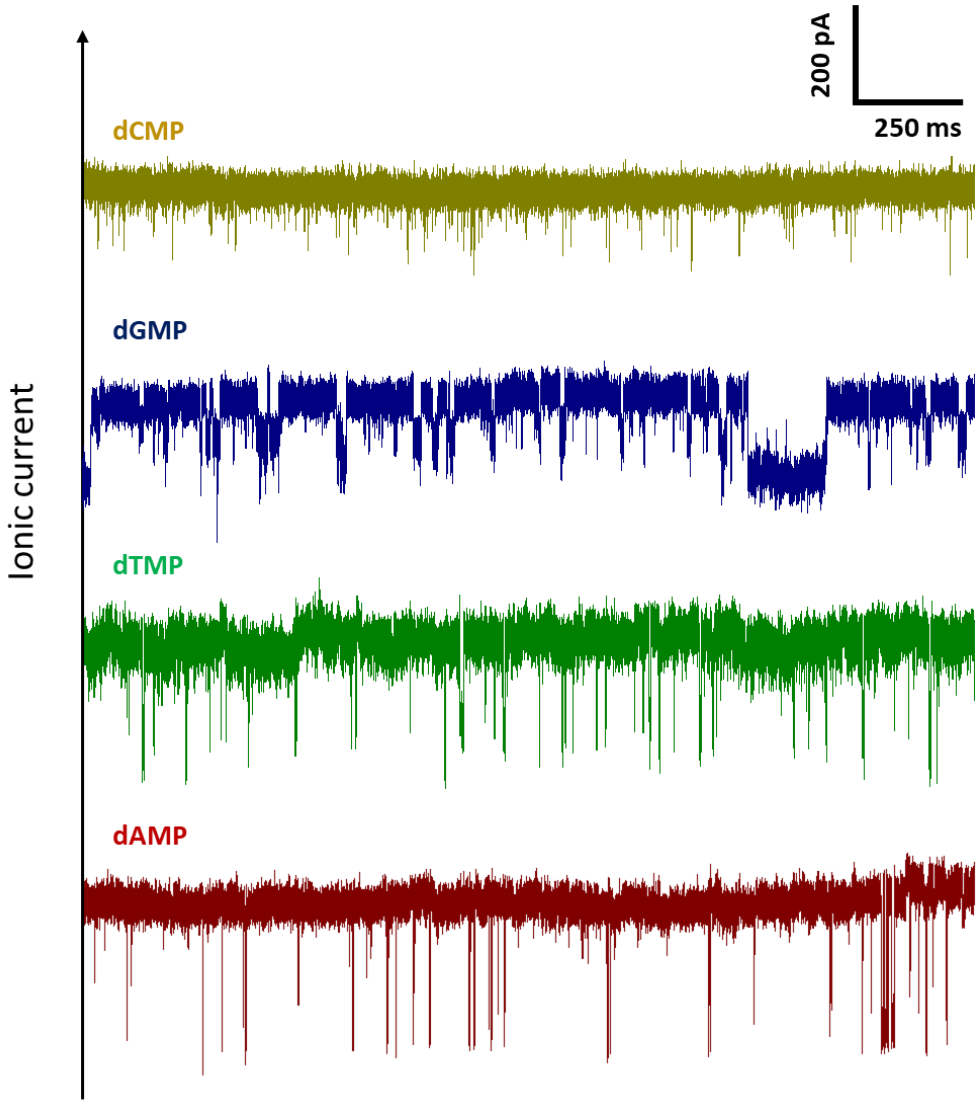

Figure S10. Typical current traces for dNMP translocation across the same single $CaCl_2$-CBD nanopore with a diameter of 1.0 nm. The solution was washed using 4 M CsCl solution buffered with 10 mM Tris-HCl at pH 7.5 after every dNMP measurement. All data were measured at an applied voltage of 0.1 V in 4 M CsCl solution buffered with 10 mM Tris-HCl at pH 7.5 (at room temperature).

SI-10. Estimation of h_{eff} of 5-nm-thick nanopore fabricated by CBD

We previously reported that an effective thickness (h_{eff}) of CBD nanopores is approximately one-third of the actual membrane thickness, similar to TEM-drilled nanopores.[9,10] Additionally, in our other previous report,[11] we confirmed the I-V characteristics of the 5-nm-thick nanopore fabricated via CBD. The measured values were well matched with the predicted line derived from Equation 1 using h_{eff} = 1.7 nm, ϕ_m = 2.8 nm (TEM-observed value). Therefore, although the shape of the CBD-made nanopore (a conical shape)[12] is different from that of the TEM-drilled nanopore (a hourglass shape)[3], we considered that the effective thickness of the 5-nm-thick CBD nanopore could be estimated to be 1.7 nm.

SI-11. I-V curves for CBD nanopores using various ions

Figure S11 shows the I-V curves for the three CBD nanopores using various ions shown in Figure 2. Figure S11 indicates that the three different nanopores have almost the same I-V characteristics in 4 M CsCl 10 mM Tris-HCl solution. This result indicates that the three different nanopores have similar sizes.

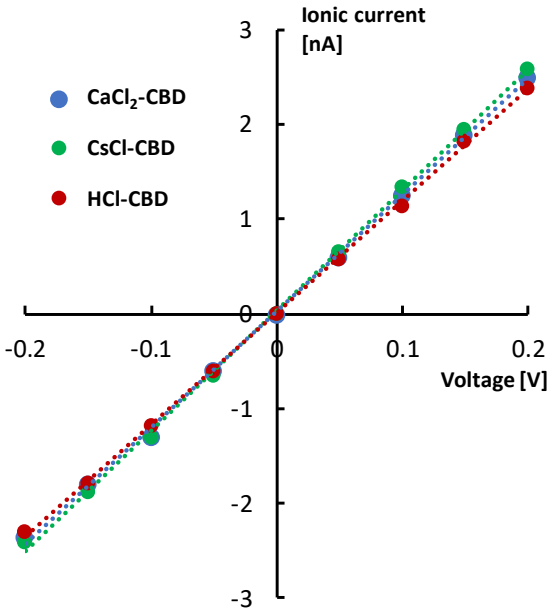

Figure S11. The I-V curves for the $CaCl_2$-CBD nanopore, CsCl-CBD nanopore and HCl-CBD nanopore are shown in Figure 2. All data were measured in 4 M CsCl solution buffered with 10 mM Tris-HCl at pH 7.5 (at room temperature).

SI-12. Ion selectivity measurements of CBD-nanopores

The adsorption of divalent ions to the nanopore wall is expected to lead to better ionic selectivity. Therefore, to estimate the Cs^+/Cl^- selectivity ratio of CBD nanopores, we performed reversal voltage measurements as described in the literature.[13] The reversal voltage V_{rev} is defined as the applied voltage at which the net current is zero. The ionic selectivity ratio was estimated for each pore by fitting the reversal voltages to the Goldman-Hodgkin-Katz (GHK) equation,

$$V_{\mathrm{rev}} = \frac{k_{\mathrm{B}}T}{e} \ln\left(\frac{S_{\mathrm{GHK}}c_{\mathrm{high}} + c_{\mathrm{low}}}{S_{\mathrm{GHK}}c_{\mathrm{low}} + c_{\mathrm{high}}}\right)$$

where S_{GHK} is the Cs^+/Cl^- selectivity ratio, c_{high} and c_{low} are the solution concentrations in the chambers, e is the electron charge, k_{B} is the Boltzmann constant, and T is the solution temperature. Since Cs^+ and Cl^- ions have similar mobilities (Cs^+: 8.01 x 10^{-4} cm^2 s^{-1} V^{-1},Cl^-: 7.92 x 10^{-4} cm^2 s^{-1} V^{-1}) [13], the liquid junction potentials (approximately < 1 mV) were negligible for these measurements.

Figure S12 shows the obtained reversal voltages for each pore. The results indicate that the Cs^+/Cl^- selectivity ratios of the $CaCl_2$-CBD nanopore and CsCl-CBD nanopore were estimated to be 3.0 x 10^2 and 6.5 x 10^1, respectively. This means that $CaCl_2$-CBD nanopores have better ionic selectivity than CsCl-CBD nanopores, which implies the adsorption of Ca^{2+} ions to the nanopore wall.

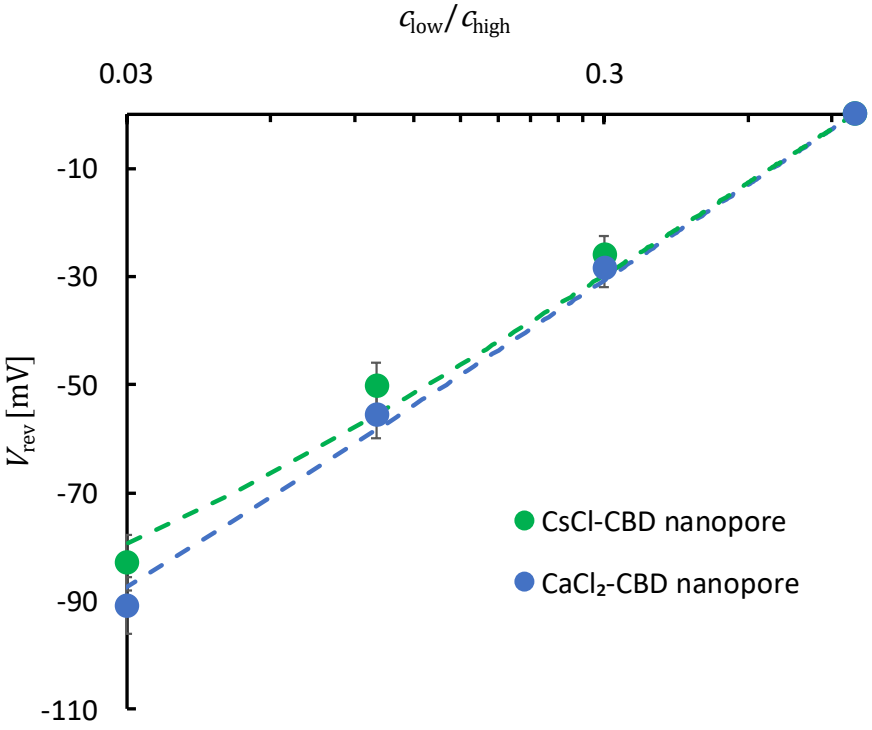

Figure S12. Reversal voltages (N=3) as a function of the concentration ratio c_{low}/c_{high}, along with fit to the GHK equation (dotted lines). c_{high}= 1 M CsCl solution, c_{low}=0.03 M, 0.1 M, 0.3 M, 1 M CsCl solution. The diameter of each pore was 1.0 nm.

References

1 I. Yanagi, T. Ishida, K. Fujisaki and K.-I. Takeda, *Sci. Rep.*, 2015, **5**, 14656.

2 R. Akahori, T. Haga, T. Hatano, I. Yanagi, T. Ohura, H. Hamamura, T. Iwasaki, T. Yokoi and T. Anazawa, *Nanotechnology*, 2014, **25**, 275501.

3 K. Venta, G. Shemer, M. Puster, J. A. Rodríguez-Manzo, A. Balan, J. K. Rosenstein, K. Shepard and M. Drndić, *ACS Nano*, 2013, **7**, 4629–4636.

4 Y. Goto, I. Yanagi, K. Matsui, T. Yokoi and K.-I. Takeda, *Sci. Rep.*, 2016, **6**, 31324.

5 S. W. Kowalczyk, D. B. Wells, A. Aksimentiev and C. Dekker, *Nano Lett.*, 2012, **12**, 1038–1044.

6 W. Saenger, *Principles of Nucleic Acid Structure*, Springer, New York, 1984.

7 S. W. Kowalczyk, M. W. Tuijtel, S. P. Donkers and C. Dekker, *Nano Lett.*, 2010, **10**, 1414–1420.

8 D. V. Verschueren, M. P. Jonsson and C. Dekker, *Nanotechnology*, 2015, **26**, 234004.

9 I. Yanagi, R. Akahori, T. Hatano and K. Takeda, *Sci. Rep.,* 2014, **4**, 5000 (2014).

10 M. Wanunu, T. Dadosh, V. Ray, J. Jin, L. McReynolds and M. Drndić, *Nat. Nanotechnol.*, **5**, 807-814 (2010).

11 Y. Goto, I. Yanagi, K. Matsui, T. Yokoi and K. Takeda, *Nanoscale*, **10**, 20844-20850 (2018).

12 C. Ying, Y. Zhang, Y. Feng, D. Zhou, D. Wang, Y. Xiang, W. Zhou, Y. Chen, C. Du and J. Tian, *Appl. Phys. Lett.*, **109**, 063015 (2016).

13 R. C. Rollings, A. T. Kuan and J. A. Golovchenko, *Nat. Commun.* **7**, 11408 (2016).